

pubs.acs.org/JPCB Article

## Proton Paths in Models of the Hv1 Proton Channel

Themis Lazaridis\*



Cite This: J. Phys. Chem. B 2023, 127, 7937-7945

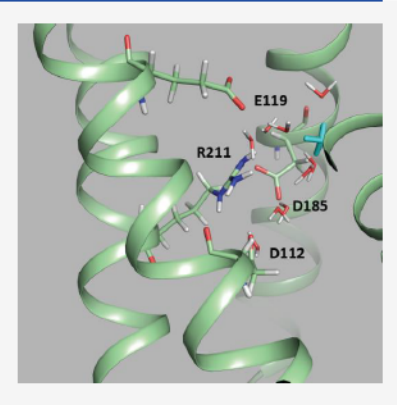


**ACCESS** I

Metrics & More

Article Recommendations

ABSTRACT: The voltage-gated proton channel (Hv1) plays an essential role in numerous biological processes, but a detailed molecular understanding of its function is lacking. The lack of reliable structures for the open and resting states is a major handicap. Several models have been built based on homologous voltage sensors and the structure of a chimera between the mouse homologue and a phosphatase voltage sensor, but their validity is uncertain. In addition, differing views exist regarding the mode of proton translocation, the role of specific residues, and the mechanism of pH effects on voltage gating. Here we use classical proton hopping simulations under a voltage biasing force to evaluate some of the proposed structural models and explore the mechanism of proton conduction. Paradoxically, some models proposed for the closed state allow for proton permeation more easily than models for the open state. An open state model with a D112–R201 salt bridge (R3D) allows proton transport more easily than models with a D112–R208 salt bridge (R2D). However, its permeation rate seems too high, considering experimental conductances. In all cases, the



proton permeates through a water wire, bypassing the salt-bridged D112 rather than being shuttled by D112. Attempts to protonate D112 are rejected due to its strong interaction with an arginine. Consistent with proton selectivity, no Na<sup>+</sup> permeation was observed in the R2D models. As a negative control, simulations with the Kv1.2–Kv2.1 paddle-chimera voltage sensor, which is not expected to conduct protons, did not show proton permeation under the same conditions. Hydrogen bond connectivity graphs show a constriction at D112, but cannot discriminate between open and closed states.

#### INTRODUCTION

The human voltage-gated proton channel (Hv1) has important physiological roles, such as acid extrusion, pH regulation in the airway epithelium, histamine release by basophils, B cell receptor signaling, and sperm mobility.1 It is homologous to voltage sensor domains (VSD) of potassium or sodium channels, but with low sequence identity.<sup>2,3</sup> Of its 273 residues, 1–80 are cytoplasmic, 95-220 make four transmembrane helices named S1-S4, and 221-273 form a coiled-coil domain, which mediates its dimerization, 4 although it can also function as a monomer. 5,6 The channel opens upon membrane depolarization, with the threshold voltage depending on the pH difference across the membrane.7 There is evidence that opening is caused by the outward movement of the S4 helix, which harbors 3 conserved arginines.<sup>8,9</sup> A solution NMR structure<sup>10</sup> and the crystal structure of a chimera between the mouse homologue, a phosphatase, and the GCN4 leucine zipper11 have been determined, but the native physiological structures of any Hv1 in the closed and open states are unknown.

The electrophysiology of Hv1 was extensively characterized even before its gene was identified. The single channel conductance is 38 fS at internal pH 6.5 and 140 fS at pH 5.5. The function of the channel was found to be quite tolerant to mutations. However, proton selectivity was lost, and the channel became anion selective when D112 near the middle of the S1 helix was mutated to a neutral residue or Lys, which led to

the proposal that D112 is the "selectivity filter". <sup>15</sup> Moving the Asp to 116, but not other locations, maintained proton selectivity. <sup>16</sup> An EPR study measured the solvent accessibility of many sites in the molecule and found that Hv1 is much more dynamic than previously studied VSDs and that a model based on the *Ciona intestinalis* (ci) VSD is in best agreement with the data. <sup>17</sup> One point of contention has been whether proton transport occurs via Grotthuss hopping along water molecules only <sup>18</sup> or titration of protein side chains is required. <sup>19</sup> The origin of the pH dependence of gating is also not settled, although the involvement of specific residues has been ascertained <sup>20</sup> and plausible hypotheses have been put forth. <sup>7</sup>

Most theoretical studies of Hv1 involved classical molecular dynamics (MD) simulations based on homology models with voltage sensors as templates.  $^{21-25}$  Calculation of the free energy profile of  $\rm H_3O^+$  through closed and open state models suggested that protonation of D112 (treated by the EVB method) could help bypass the major electrostatic barrier.  $^{26}$  QM/MM simulations observed excess protons protonating different

Received: June 12, 2023 Revised: August 14, 2023 Published: September 11, 2023





clusters of Asp/Glu residues, and classical metadynamics showed proton transport, especially in the presence of two protons. PFT geometry optimizations of a reduced model in a dielectric continuum found that the proton was able to protonate a salt-bridged Asp, but other ions were excluded. Constant-pH MD studies have attempted to identify the residues involved in pH sensing. One key issue is the magnitude of the movement of the S4 helix; some models of the open state have D112 paired with R211 (R3D models), which implies a movement of two helical turns, 21,25,31,32 and others with R208 (R2D models), which implies a movement of one helical turn. T7,22,33 The closed state is usually modeled with a D112–R205 salt bridge (R1D), but not always. The pairing of D112 is a main differentiating feature of homology models, but there can be other differences between them.

In this work we use an algorithm for performing classical MD with proton hopping between waters and/or protein side chains.<sup>34</sup> We consider four models each of the closed and open states. A voltage biasing force is used to drive protons from one side of the membrane to the other in an accessible simulation time, and the paths that the proton takes are examined. Comparison between the models allows us to draw some conclusions about the validity of the models and the mechanism of proton conduction.

#### METHODS

The following structures were considered: the NMR structure of Hv1 in detergent micelles10 (NMR, pdb code 5OQK), the alphafold (AF2) predicted structure of Hv1 (alphafold.ebi.ac. uk/entry/Q96D96), the chimeric mouse-phosphatase crystal structure<sup>11</sup> (chim, pdb code 3WKV), the closed (R1D) and open (R3D) models of Hv1 from Geragotelis et al. 25 (gerC and gerO, respectively), an R2D model for the open state of Hv1<sup>35</sup> (banh), and two homology models of Hv1 created here, one based on the ciVSD open state, pdb 4G7V36 (ciOP), and one based on the structure of the paddle-chimera VSD<sup>37</sup> (2R9R). The latter two are models of the open state and were created using Modeller.<sup>38</sup> For the first one (R2D), we used the alignment of Li et al., 17 and for the second (R2/3D) the alignment of Chamberlin et al.<sup>23</sup> Most Hv1 systems included residues 88-230, except 4G7V (98-218) and 2R9R (93-220). The chimera included residues 84-225, with missing loops built using the SuperLooper2 Web site.<sup>39</sup> Figure 1 gives an overview of the 8 starting structures. Control simulations were also done with the paddle-chimera voltage sensor, which is a hybrid from the Kv1.2 and Kv2.1 potassium channels (pdb 2R9R). We are not aware of electrophysiology experiments on this artificial domain, but the similar Shaker K+ VSD was found not to conduct protons. 40,41

A membrane of 104 POPC lipids was constructed around the 2R9R homology model using the charmm-gui server <sup>42</sup> and equilibrated using its standard protocol (i.e., three cycles of 25 ps each and three cycles of 50 ps each, with gradually diminishing harmonic restraints on protein backbone, side chains, lipids, and water, followed by 10 ns unrestrained MD). The other models were inserted into the equilibrated 2R9R system by aligning and replacing the protein and re-equilibrating (energy minimization for 10000 steps and MD simulation for 200 ps using a harmonic restraint of 1 kcal/mol/Ų for the protein). All systems had 5858 TIP3P water molecules, 5 chloride ions, and 5 protonatable waters (except 2R9R which had 20 protonatable waters, no chloride, and 5848 TIP3P) in a box of about  $62 \times 62 \times 85$  Å. The net charge of the unit cell depends on the protonation states and

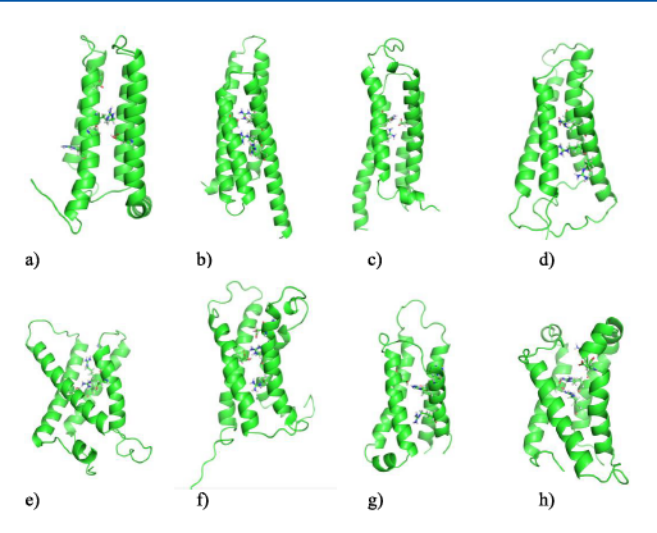


Figure 1. Starting structures of the 8 models considered: (a) NMR, (b) AF2, (c) chim, (d) gerC, (e) gerO, (f) banh, (g) ciOP, and (h) 2R9R. The three Arg, D112, and D185 are in stick representation.

the number of protons and varies between 0 and +3. A small net charge in the unit cell does not have noticeable effects on proton transport. <sup>43</sup> The charmm36 force field for the protein <sup>44</sup> and the lipids <sup>45</sup> was used. The simulations were run at a constant temperature of 303 K and a constant pressure of 1 bar using the Nose-Hoover and Langevin piston methods. The time step was 2 fs and the van der Waals cutoff 12 Å. Particle Mesh Ewald <sup>46</sup> was used for long-range electrostatics. The membrane is parallel to the xy plane.

The excess proton was modeled as a classical hydronium. The proton hopping simulations were carried out with the MOBHY module of the CHARMM package. Every 10 steps, an attempt is made to move a proton from the current  $H_3O^+$  to a water molecule or a protein side chain that is hydrogen bonded to it. When an attempt is made to protonate a TIP3P molecule, the latter is switched with a protonatable water (i.e., one with a dummy third hydrogen). Harmonic restraints were used to keep the membrane-protein system at the center of the box, the protein at a certain point in the xy plane, and the protonatable waters in a 5 Å cylinder around the channel axis and within  $\pm 34$  Å from the membrane center (to prevent them from crossing periodic boundaries). The proton concentration within this cylinder is about 1 M, therefore the effective pH is  $\sim 0$ .

To accelerate proton transport we used voltage, which was applied in a 55 Å wide region across the membrane<sup>49</sup> and felt only by the hydronium, the protonatable water molecules, and the titratable side chains (otherwise the membrane would be destabilized by the high voltage used). We confirmed that voltage does not affect the conformation and orientation of the short Asp side chains (it did affect the longer Arg side chains whenever they were included, not in the results reported here). We only consider outward currents because with inward pH gradients the channel is closed,<sup>50</sup> although the open channel conducts in both directions. The voltage was empirically chosen as the smallest possible that allows proton conduction to be observed over the 0.5 ns duration of the simulations. The duration of the simulations was kept short so as to limit the variance of the first passage times and allow statistically significant differences to be observed (see the Supporting Material of ref 43). In the simulations, certain side chains were chosen as titratable (usually D112 and D185). Whether a side chain will protonate/deprotonate or not depends on the

empirical hopping thresholds established in bulk water simulations.<sup>34</sup> The thresholds used here are (in kcal/mol) 20 for hydronium-water transfer, 24 for Asp to water transfer, and 20 for water to Asp.

The hydrogen bonding connectivity was calculated using the Bridge2 program, <sup>51</sup> which analyzes MD trajectories and identifies H-bonding connections between protein residues. Connectivity graphs were generated either for the protein side chains, allowing a water bridge length of 5, or for the pore waters. In the former case, the first trajectory at 3 V was used as input for each model. In the latter case, only the initial structure was used as input after deleting all lipids and protein atoms as well as solvent with |z| coordinates larger than 12 Å. The default criteria were used for an H bond (3.5 Å, 60°).

#### RESULTS

For each model, two sets of five runs were executed and reported separately to give a sense of the statistical uncertainty. Table 1

Table 1. Summary of the Systems and Conditions Studied and Results Obtained a

		2 V	3 V	5 V
NMR	"closed"	0,0	1,1	
AF2	"closed"		0,0 (1,0)	2,1 (2,3)
chim	"closed"		0,0 (0,1)	1,2 (3,3)
gerC	"closed"	1,0	2,2	
gerO	"open"	0,0	2,2	
banh	"open"		0,0 (1,0)	0,0 (2,3)
ciOP	"open"		0,0 (1,0)	0,1 (4,4)
2R9R	"open"		0,0 (2,3)	2,2 (5,5)
gerO/Na <sup>+</sup>	"open"		0,0	2,0
banh/Na+	"open"		0,0	0,0

"The heads of the columns give the biasing voltage. The purported state of the channel is indicated in the second column. The numbers indicate the number of runs out of five that led to channel crossing by the proton (two sets of five were run). Numbers in parentheses are for acidic residues in the inner vestibule protonated. All runs lasted 0.5 ns.

reports the number of runs out of five in which the proton crosses the channel, i.e., attains a z coordinate above +20 Å. In the remaining runs, the proton may be in the inner vestibule, in the central region, or in the outer vestibule. These differences, which are also informative on the permeability of the channel, are not reported in Table 1 but described in the text. Because it was often observed that the proton was stuck interacting with acidic residues in the inner vestibule (e.g., E153 or E164, D171, D174), additional runs were done with these residues protonated (values in parentheses in Table 1). This fully protonated state is used as an extreme case scenario that favors maximal conductance. Further systematic study is needed to elucidate the impact of each of these residues on conductance together with estimates of protonation/deprotonation kinetics (see Discussion).

The NMR structure of a truncated 80–226 Hv1 in LDAO/DPC mixed micelles was determined with Zn<sup>2+</sup>, which is known to stabilize the closed state. This structure differs significantly from homology models. The helices are straight and parallel, and the side chains are not well packed in the interior. Especially F150, V109, V177, and V178, which are thought to form a "hydrophobic gasket", are very far from each other. The positions of the three Arg residues could not be ascertained with confidence in the experiments. R205 is close but not salt-bridged

with D112 and the other two Arg also do not form salt bridges. Our results confirm that this structure is more permeable compared with other models. Out of ten runs at 3 V, in two the proton crosses the channel completely. In three other runs it gets to the central region of the channel, and in two more it gets to the outer vestibule. The path of the proton runs close to D185, which is protonated once but deprotonates right away. At 2 V the proton fails to enter the inner vestibule except in one out of ten runs.

The AF2 prediction is similar to homology models. D112 is salt-bridged with R205, and Arg 208 below interacts with D185. F150 is packed against R208 and is close to V109 but far from V177 and V178. At 3 V and most of the 5 V runs, the proton is stuck between D174 and R211. Protonating D174, D171, and E164, the proton moves higher, but further progress is blocked by F150—R208. One of ten runs at 3 V shows the proton fully crossing the channel. Raising the voltage to 5 V allowed five of the runs to cross. In one of these runs, D185 gets protonated transiently, and in the other four, no protonation takes place. In four of the noncrossing runs, the proton is found in the central region, and in one the proton is found in the inner vestibule.

The chimera crystal structure is unusual in that it features two hydrophobic barriers with an 8 Å cavity between them. The lower layer includes (mouse numbering, add 4 for human Hv1) F146, L150, F178, and R204 and the upper layer V112, L197, L143, and L185. It is thought to be in an intermediate-resting conformation and closed, because of the presence of Zn²+, and has D108 between R1 and R2. It was shown to be proton-selective and voltage-activated but with altered characteristics compared to the wild-type mouse channel. Runs at 3 V show the proton stuck at Asp/Glu residues on the intracellular side. Protonation of these residues allows crossing in one of ten runs. At 5 V six of the ten runs show proton crossing, and in the other four the proton ends up in the central region, in two of them protonating D108 or D181.

The "closed" structure of Geragotelis et al. 25 (gerC) was obtained by starting from a homology model based on the chimera crystal structure and applying negative, hyperpolarizing voltage. R205 is salt-bridged to both D112 and D185, and R208 is salt-bridged to E153. However, the structure leaves quite a bit of space for water and protons to move through. Indeed, ten runs at 3 V show four complete proton crossings. In the remaining six runs, the proton ends up in the central region or outer vestibule, sometimes protonating D185 and less often D112. In two of the four complete crossings, D185 gets protonated transiently, and in the other two, no protein residue gets protonated at all. At 2 V, in one of ten runs, the proton crosses the channel completely, and in the remaining ones it ends up at various places in the channel interior.

The "open" structure of Geragotelis et al. 25 (gerO) was obtained by applying positive voltage. It matches D112 with R211 and so belongs to the R3D class. This structure has similar permeability to gerC. At 3 V, four of the ten runs show complete crossing, and in the remaining six, the proton ends up in the central region or outer vestibule. Even at 2 V most runs allow the H<sup>+</sup> to get into the central region. In the crossing trajectories, D112 is transiently protonated, but this is not essential for conduction. Escape outward happens around the D112–R211 salt bridge (see below).

The homology model of Banh et al. <sup>22,35</sup> belongs to the R2D class, i.e., it has D112 salt-bridged to R208. This structure is less easy to cross than the R3D model above because R3 imposes an extra barrier to the proton. Only with acidic residues protonated

do we observe one crossing at 3 V and five crossings at 5 V out of 10 runs. In the other runs, the proton stays mostly below R3. In the crossing trajectories, D185 or D112 are transiently protonated or no protonation takes place.

ciOP is an R2D homology model constructed using ci-VSD open state as a template and the alignment proposed by Li et al. <sup>17</sup> It is very similar to banh, except R208 interacts more strongly with D185 than D112. According to Table 1, this model is somewhat more permeable than banh. With acidic residues protonated, 8 out of 10 trajectories show complete crossing, most of them without any protonation. At 3 V only one out of 10 runs shows proton permeation in which D112 is transiently protonated.

The final model was built on 2R9R using the alignment of Chamberlin et al.<sup>23</sup> and matches D112 with R2 and R3. This model exhibits a somewhat higher permeability than the other R2D open state models.

To address the issue of ion selectivity, we considered Na<sup>+</sup> conduction in the gerO and banh models. For gerO at 3 V, when H<sup>+</sup> permeates easily, sodium gets stuck either below the E153–R223 salt bridge or below the D185–D112–R211 triplet. At higher voltage, however, it does manage to push through in two of the ten runs. The banh structure shows lower permeability to Na<sup>+</sup>, since no conduction was observed at either 3 or 5 V. These results are qualitatively consistent with proton selectivity, but quantitative confirmation of the experimental >10<sup>6</sup> selectivity for H<sup>+</sup> vs Na<sup>+12</sup> is not possible with the present approach. Observing no Na<sup>+</sup> conduction in a few short runs is a necessary but not sufficient condition for agreement with experiment.

As a negative control, we performed similar simulations on the paddle-chimera voltage sensor (pdb 2R9R). Out of ten runs each at 5 and 9 V, only one proton conduction was observed at 9 V. The proton usually got stuck in a cavity formed by E226, R296, E183, and D220.

How the Salt Bridge is Bypassed in the R3D and R2D **Models.** In the results presented above, we often observed proton permeation without titration of any protein residue. In a subset of crossing runs, transient protonation of either D112 or D185 took place. We looked at the mechanism of proton permeation in several trajectories and present here as a representative example how the crossing of the main barrier, i.e., the D112-Arg salt bridge, takes place in one of the gerO runs at 2 V. Figure 2 shows four snapshots from the point when crossing around R211 takes place. In Figure 2a (step 185 K) the H<sub>3</sub>O<sup>+</sup> is interacting with D112. Between steps 142 and 192 K many attempts to protonate D112 occur, but all are rejected due to a high energy gap. Even if D112 was protonated, it would not be able to shuttle the proton because both carboxylic oxygens are below R211. At step 192.1K the proton moves away from D112 (Figure 2b) and at 192.5K higher up (Figure 2c). At step 195.6K, it starts interacting with E119, which is above R211. These hops around R211 are aided by the voltage, which lowers the hopping energy in the outward direction.

All R2D models we considered are less permeable than the R3D model because R3 poses an additional barrier to a proton moving outward. We looked more closely at the banh structures at 3 V with the acidic residues protonated. In most runs, the proton remains below R3, near or below D171 (Figure 3a). In the one run in which it crosses the channel, it first passes R3 (Figure 3b) and then R2 (Figure 3c). Despite many attempts, D112 gets protonated only transiently, twice, and that does not help conduction. In the end the proton goes around R2 on the other side, between R2 and D185, which is at about 6 Å distance.

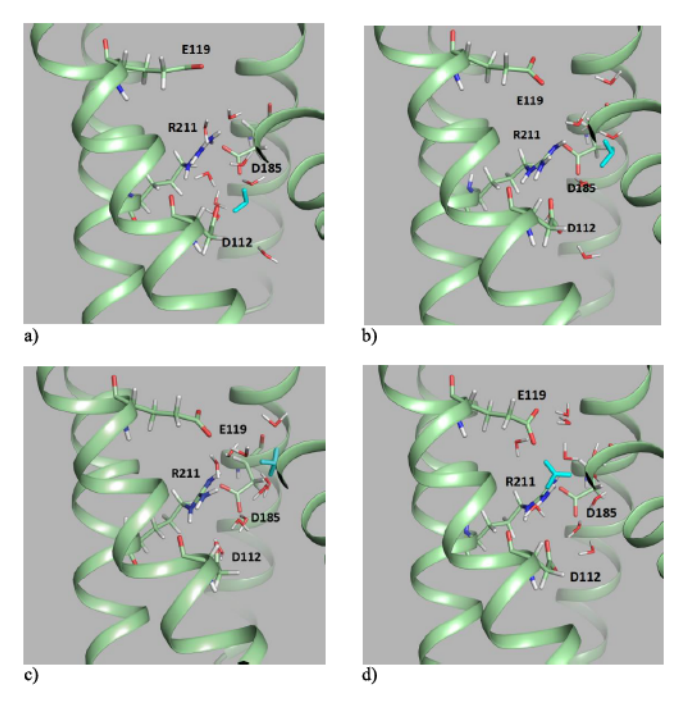


Figure 2. Snapshots from bypassing R211–D112–D185 in gerO;  $\rm H_3O^+$  is in cyan: (a) step 185K; (b) step 192.1K; (c) step 192.5K; (d) step 195.6K.

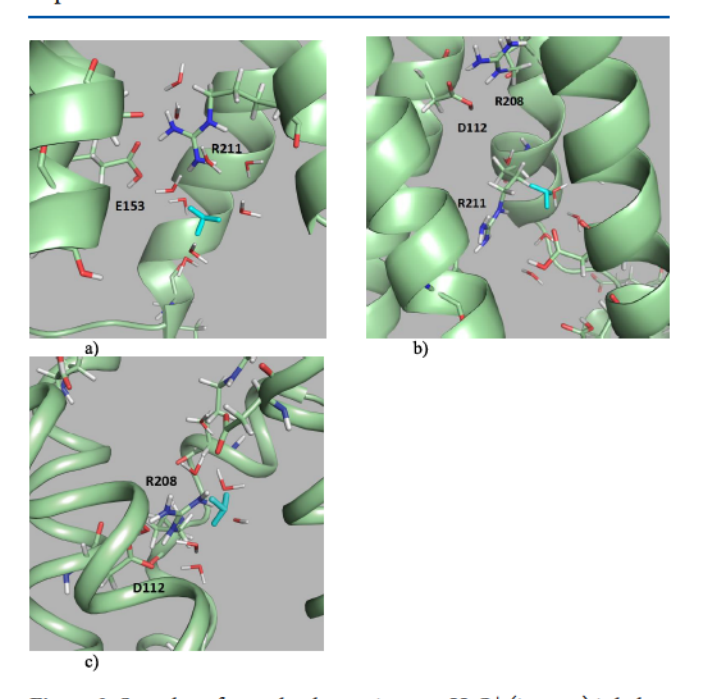


Figure 3. Snapshots from a banh crossing run.  $\rm H_3O^+$  (in cyan) is below R211 in (a), bypasses R211 in (b), and bypasses R208 in (c).

D185 does not get protonated but the energy gaps are just above the threshold. These events are representative for all permeation events in R2D channels.

Hydrogen Bonding Connectivity. Proton transfer ability is commonly judged by the existence of a hydrogen-bonded chain of water molecules and protein side chains. We used the program Bridge2<sup>51</sup> to create graphs of hydrogen bond networks between protein side chains in the eight models considered (Figure 4). In this graph, H bonding protein residues are represented by nodes. An edge between two nodes is depicted if

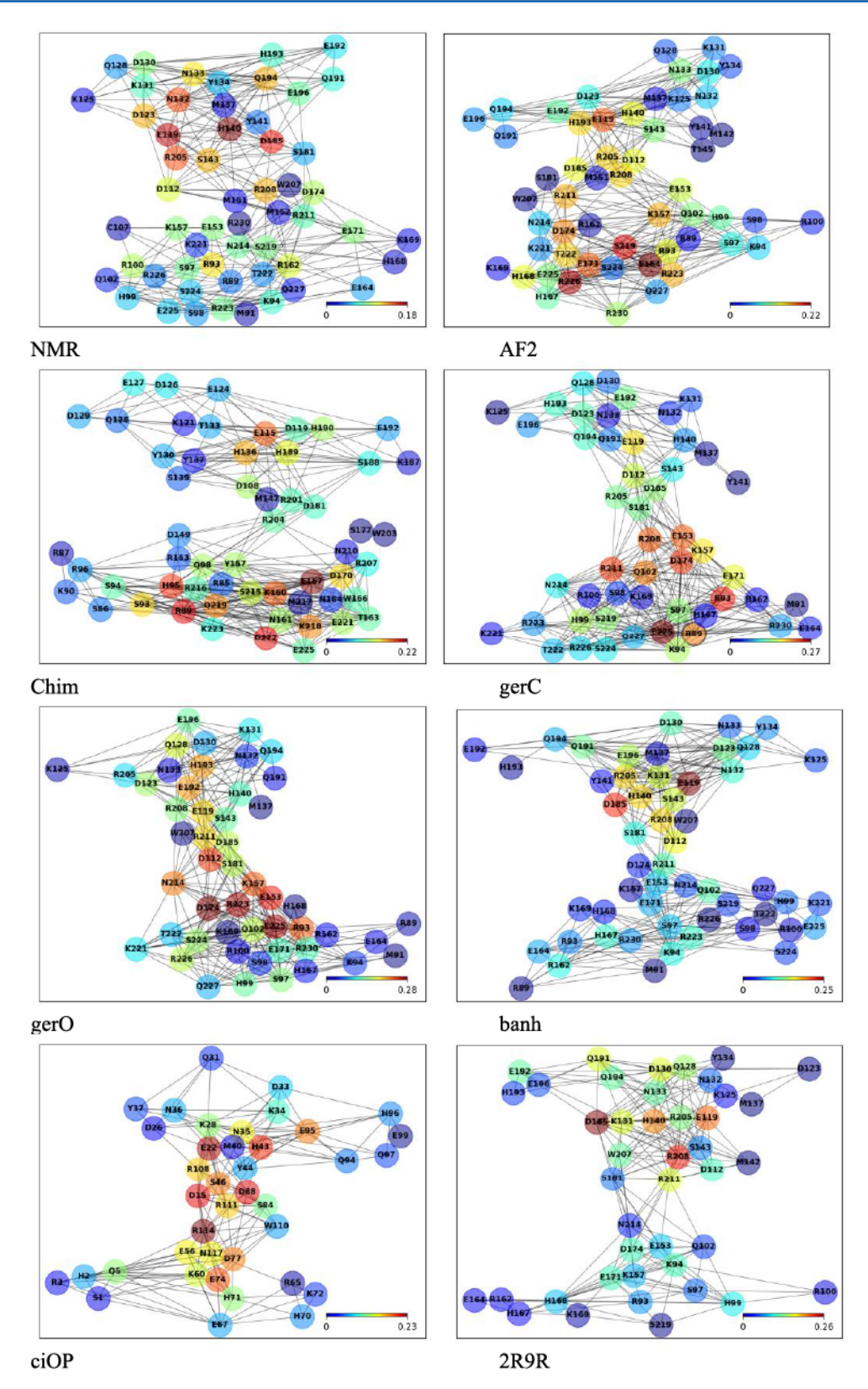


Figure 4. Hydrogen bond connectivity between protein side chains in the starting structure of the 8 models calculated using the program Bridge2. The coloring is based on the number of edges around each node ("degree centrality").

the residues are connected by 5 water molecules or less. All models show a constriction near the critical D112 residue, but there is no large difference between "open" and "closed" models. It is difficult to rationalize the results in Table 1 based on these

graphs. For example, looking at the graphs for gerC, gerO, and ciOP, it would be difficult to predict that the latter is much less permeable than the first two.

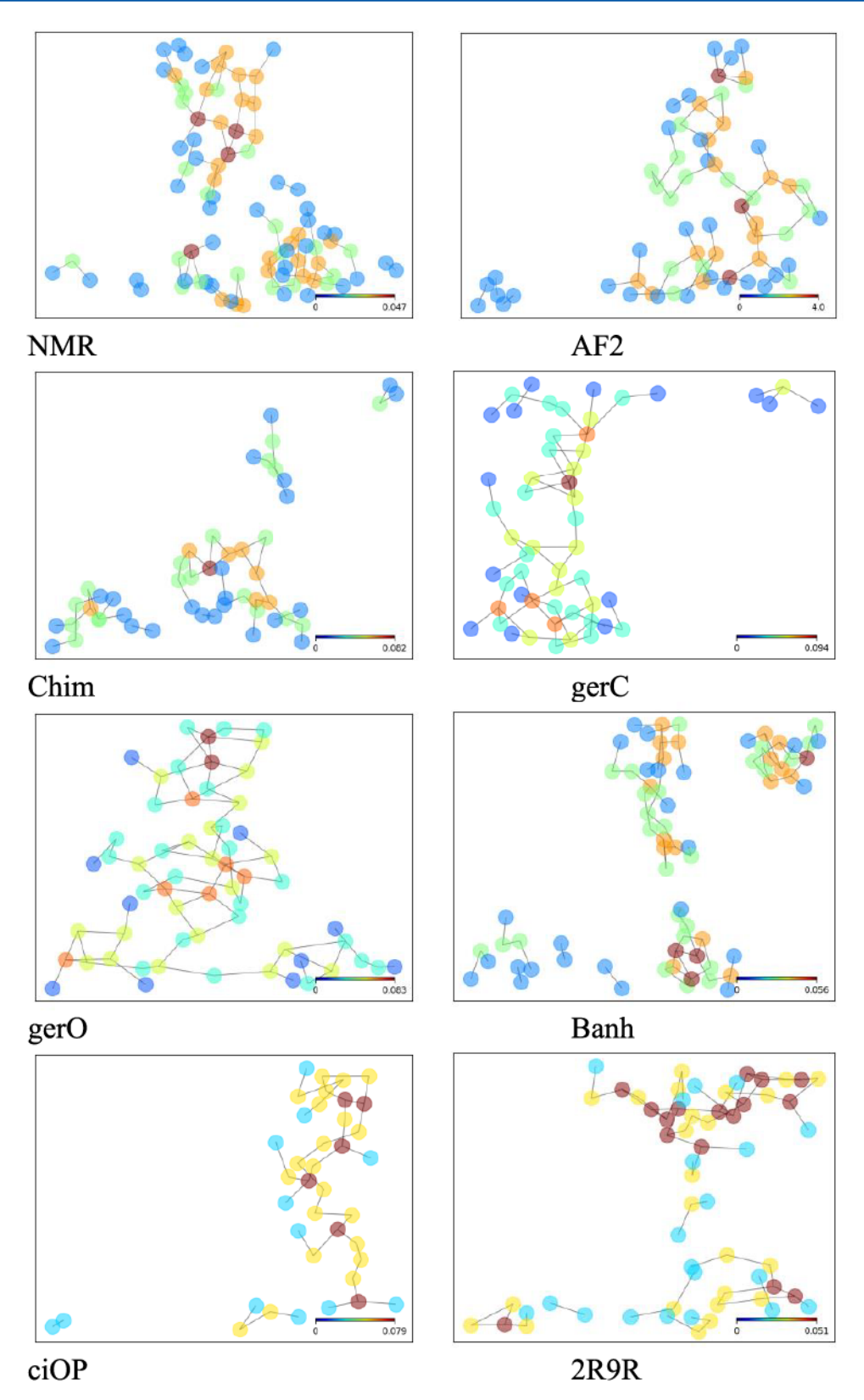


Figure 5. Hydrogen bond connectivity between pore waters in the starting structure of the 8 models calculated using the program Bridge2.<sup>51</sup> The coloring is based on the number of edges around each node ("degree centrality").

We also computed H bond networks between pore water molecules (Figure 5). These graphs do exhibit some correlation with the facility of  $H^+$  transport because they correlate with hydration. For example, the most connected graph is for gerO,

which is also the most permeable. But the correlation is not perfect. For example, the NMR structure is disconnected, but it is very easily permeable. The 2R9R model is very disconnected, but it is slightly more permeable than ciOP which is connected.

It should be noted that these graphs are for the initial structure and there may be variability during the trajectory. A pair of water molecules that is not H bonded in one frame may become H bonded in a different frame. Averaging over frames is difficult because the water molecules exchange with each other.

### DISCUSSION

In this work, we applied a novel approach to investigate proton permeation paths in the human Hv1 proton channel. It uses classical simulations with periodic attempts to move a proton along H bonds and an empirical threshold-based criterion for accepting a proton hop. This approach has the advantages of including a proton explicitly in the modeling and considering the dynamics and energetics of proton movement. The main disadvantage is that the approach is empirical and qualitative. No calculation of conductance is made in these runs, only a comparison between models at similar conditions. An artificially strong biasing force is used to accelerate proton permeation and that could distort the pathway the proton takes. Therefore, these results should be viewed with caution and ideally confirmed by more rigorous methods. To say whether a channel is open or closed, we should calculate proton transport rates, i.e., identify the critical barriers and determine the extent to which they are lowered by the biasing force. This is a difficult task that remains a long-term goal. A step in that direction has been made for side chain protonation and deprotonation.

Despite the limitations, some judgments can be made concerning the various models proposed. Some structures that were proposed to be closed turn out to be more permeable, according to the present study, than the purportedly open models. For example, the NMR structure in micelles is too easily permeated by protons. This is not surprising given the loose packing and the lack of salt bridges in this structure. The proposed closed structure of Geragotelis et al.<sup>25</sup> is also too permeable. The same conclusion was reached by looking at the pore dimensions.<sup>53</sup> Perhaps the voltage that was applied in the MD simulation caused a transient opening of the structure, which then did not have enough time to relax. Concerning the open state models, we can safely say that the one R3D model (gerO) is much more easily permeable than the several R2D models we have considered. To choose between the two, we would need either an estimate of the conformational free energy of the two models at a given voltage or an estimate of the time scale of permeation.

A rough estimate of the expected time to cross an open Hv1 channel could perhaps be made by assuming that the experimental conductances extrapolate linearly to very large voltages, that our artificial voltage biasing force exerts similar effects as the physiological voltage, and that the rate limiting step is in the crossing of the channel rather than diffusional approach to it. The largest experimental conductance calculated is 140 fS at internal pH 5.5. This corresponds to  $0.875 \times 10^{-3}$  protons/nsV, or  $1.10~\mu$ s/proton at 1 V, or 220 ns/proton at 5 V. Thus, observing proton crossings on the time scale of 1 ns is too fast. From this point of view, the R2D models are closer to the expected speed of translocation than the R3D model, where translocation was facile even without protonating the inner vestibule Asp residues.

One of the debates in the Hv1 field is whether proton conduction takes place via a water wire <sup>18</sup> or by shuttling through the D112 residue. <sup>19</sup> There are cogent arguments in favor of both mechanisms. In the present simulations, we have not observed any case of shuttling by the D112 residue. Most attempts to

protonate D112 are rejected (it interacts closely with an Arg) and even when D112 gets protonated it does not shuttle the proton because in the present structures D112 does not straddle the Arg, but lies below it. Instead, the proton passes around the Arg through a water wire. It should be noted, of course, that whether protonation will take place or not in our simulations depends on energy gap thresholds established by simulations in bulk water.<sup>34</sup> This approach can give only a rough estimate. The conclusions need to be confirmed by more detailed calculations and/or quantum mechanical calculations. In that regard, a quantum mechanical study of a reduced system found that a hydronium approaching a D-R salt bridge will protonate the Asp whereas a different ion will be rejected.<sup>28</sup> Although quantum mechanics is clearly superior to classical methods, that quantum mechanical study also has some caveats: it neglected the protein surroundings and hydrating water, which would stabilize the charged species and keep the D112 p $K_a$  low. A normal p $K_a$  for D112 was found in a recent constant pH MD study. 30 Normal  $pK_a$ s were also found experimentally for a buried Glu-Arg pair in staphyloccocal nuclease.53

If Asp does not need to be protonated, what is the origin of the proton selectivity compared to Na<sup>+</sup>? We observed that shuttling of the proton by Asp is not necessary to obtain selectivity. Grotthuss hopping allows water molecules to transfer a proton without being at the top of a free energy barrier but merely close enough to H-bond to another water molecule on the other side of the barrier (about 1.5 Å from the top of the barrier. This could reduce the effective barrier significantly (we could perhaps term this effect "Grotthuss tunneling"). Whether this is enough to explain the observed selectivity should be addressed with a more quantitative analysis.

Another argument in favor of the shuttling hypothesis was that no water permeability is observed. <sup>53</sup> However, it is not clear whether water-wire transport must always be associated with water movement. This issue needs to be further investigated in the future. Other interesting possibilities for future work are the R205H mutant of Hv1, which was found to conduct protons in the resting state, albeit at substantially lower rates. <sup>32</sup> Proton conduction was also observed for the R  $\rightarrow$  H mutants of voltage sensors <sup>56</sup> and is thought to occur via His shuttling. The N214R—R205H double mutant, which exhibits inward rectification, would also be interesting to study, as well as the Hv1 mutants that were found to be anion-selective. <sup>15</sup>

An EPR study found that Hv1 is much more dynamic than previously studied VSDs. <sup>17</sup> It is thus a possibility that the protein samples a wide range of conformations, only some of which allow proton permeation. In that case, no single structure can represent the open state of the channel; instead, one should work with an ensemble of conformations. Producing such an ensemble, either experimentally or computationally, is very challenging.

#### AUTHOR INFORMATION

#### **Corresponding Author**

Themis Lazaridis — Department of Chemistry, City College of New York/CUNY, New York, New York 10031, United States; Graduate Programs in Chemistry, Biochemistry, and Physics, The Graduate Center, City University of New York, New York, New York 10016, United States; orcid.org/0000-0003-4218-7590; Phone: (212) 650-8364; Email: tlazaridis@ccny.cuny.edu

Complete contact information is available at:

https://pubs.acs.org/10.1021/acs.jpcb.3c03960

#### Notes

The author declares no competing financial interest.

#### ACKNOWLEDGMENTS

We thank the National Science Foundation (MCB-1855942) for funding and Dr. R. Pomes for providing the coordinates of the banh model.

#### REFERENCES

- (1) DeCoursey, T. E. Voltage-Gated Proton Channels: Molecular Biology, Physiology, and Pathophysiology of the HV Family. *Physiol. Rev.* 2013, 93, 599–652.
- (2) Sasaki, M.; Takagi, M.; Okamura, Y. A Voltage Sensor-Domain Protein Is a Voltage-Gated Proton Channel. *Science* 2006, 312, 589–592.
- (3) Ramsey, I. S.; Moran, M. M.; Chong, J. A.; Clapham, D. E. A Voltage-Gated Proton-Selective Channel Lacking the Pore Domain. *Nature* 2006, 440, 1213–1216.
- (4) Lee, S. Y.; Letts, J. A.; MacKinnon, R. Dimeric Subunit Stoichiometry of the Human Voltage-Dependent Proton Channel Hv1. *Proc. Natl. Acad. Sci. U. S. A.* 2008, 105, 7692–7695.
- (5) Koch, H. P.; Kurokawa, T.; Okochi, Y.; Sasaki, M.; Okamura, Y.; Larsson, H. P. Multimeric Nature of Voltage-Gated Proton Channels. *Proc. Natl. Acad. Sci. U. S. A.* 2008, 105, 9111–9116.
- (6) Tombola, F.; Ulbrich, M. H.; Isacoff, E. Y. The Voltage-Gated Proton Channel Hv1 Has Two Pores, Each Controlled by One Voltage Sensor. *Neuron* 2008, 58, 546–556.
- (7) Sokolov, V. S.; Cherny, V. V.; Ayuyan, A. G.; DeCoursey, T. E. Analysis of an Electrostatic Mechanism for ΔpH Dependent Gating of the Voltage-Gated Proton Channel, HV1, Supports a Contribution of Protons to Gating Charge. *Biochim. Biophys. Acta Bioenerg.* 2021, 1862, No. 148480.
- (8) Gonzalez, C.; Koch, H. P.; Drum, B. M.; Larsson, H. P. Strong Cooperativity between Subunits in Voltage-Gated Proton Channels. *Nat. Struct. Mol. Biol.* 2010, 17, 51–57.
- (9) Gonzalez, C.; Rebolledo, S.; Perez, M. E.; Larsson, P. P. Molecular Mechanism of Voltage Sensing in Voltage-Gated Proton Channels. *J. Gen. Physiol.* 2013, 141, 275–285.
- (10) Bayrhuber, M.; Maslennikov, I.; Kwiatkowski, W.; Sobol, A.; Wierschem, C.; Eichmann, C.; Frey, L.; Riek, R. Nuclear Magnetic Resonance Solution Structure and Functional Behavior of the Human Proton Channel. *Biochemistry* 2019, 58, 4017–4027.
- (11) Takeshita, K.; Sakata, S.; Yamashita, E.; Fujiwara, Y.; Kawanabe, A.; Kurokawa, T.; Okochi, Y.; Matsuda, M.; Narita, H.; Okamura, Y.; et al. X-Ray Crystal Structure of Voltage-Gated Proton Channel. *Nat. Struct. Mol. Biol.* 2014, 21, 352–357.
- (12) Decoursey, T. E. Voltage-Gated Proton Channels and Other Proton Transfer Pathways. *Physiol. Rev.* 2003, 83, 475–579.
- (13) Cherny, V. V.; Murphy, R.; Sokolov, V.; Levis, R. A.; DeCoursey, T. E. Properties of Single Voltage-Gated Proton Channels in Human Eosinophils Estimated by Noise Analysis and by Direct Measurement. *J. Gen. Physiol.* 2003, 121, 615–628.
- (14) Ramsey, I. S.; Mokrab, Y.; Carvacho, I.; Sands, Z. A.; Sansom, M. S. P.; Clapham, D. E. An Aqueous H + Permeation Pathway in the Voltage-Gated Proton Channel Hv1. *Nat. Struct. Mol. Biol.* 2010, *17*, 869–875.
- (15) Musset, B.; Smith, S. M. E.; Rajan, S.; Morgan, D.; Cherny, V. V.; Decoursey, T. E. Aspartate 112 Is the Selectivity Filter of the Human Voltage-Gated Proton Channel. *Nature* 2011, 480, 273–277.
- (16) Morgan, D.; Musset, B.; Kulleperuma, K.; Smith, S. M. E.; Rajan, S.; Cherny, V. V.; Pomès, R.; DeCoursey, T. E. Peregrination of the Selectivity Filter Delineates the Pore of the Human: Voltage-Gated Proton Channel HHv1. *J. Gen. Physiol.* 2013, 142, 625–640.
- (17) Li, Q.; Shen, R.; Treger, J. S.; Wanderling, S. S.; Milewski, W.; Siwowska, K.; Bezanilla, F.; Perozo, E. Resting State of the Human

- Proton Channel Dimer in a Lipid Bilayer. Proc. Natl. Acad. Sci. U. S. A. 2015, 112, E5926—E5935.
- (18) Bennett, A. L.; Ramsey, I. S. CrossTalk Opposing View: Proton Transfer in Hv1 Utilizes a Water Wire, and Does Not Require Transient Protonation of a Conserved Aspartate in the S1 Transmembrane Helix. *J. Physiol.* 2017, 595, 6797—6799.
- (19) DeCoursey, T. E. CrossTalk Proposal: Proton Permeation through HV1 Requires Transient Protonation of a Conserved Aspartate in the S1 Transmembrane Helix. *J. Physiol.* 2017, 595, 6793–6795.
- (20) Cherny, V. V.; Morgan, D.; Thomas, S.; Smith, S. M. E.; DeCoursey, T. E. Histidine168 Is Crucial for  $\Delta pH$ -Dependent Gating of the Human Voltage-Gated Proton Channel, HHV1. *J. Gen. Physiol.* 2018, 150, 851–862.
- (21) Wood, M. L.; Schow, E. V.; Freites, J. A.; White, S. H.; Tombola, F.; Tobias, D. J. Water Wires in Atomistic Models of the Hv1 Proton Channel. *Biochim. Biophys. Acta Biomembr.* 2012, 1818, 286–293.
- (22) Kulleperuma, K.; Smith, S. M. E.; Morgan, D.; Musset, B.; Holyoake, J.; Chakrabarti, N.; Cherny, V. V.; DeCoursey, T. E.; Pomès, R. Construction and Validation of a Homology Model of the Human Voltage-Gated Proton Channel HH <sub>V</sub> 1. *J. Gen. Physiol.* 2013, 141, 445–465.
- (23) Chamberlin, A.; Qiu, F.; Rebolledo, S.; Wang, Y.; Noskov, S. Y.; Larsson, H. P. Hydrophobic Plug Functions as a Gate in Voltage-Gated Proton Channels. *Proc. Natl. Acad. Sci. U. S. A.* 2014, 111, E273–E282.
- (24) Gianti, E.; Delemotte, L.; Klein, M. L.; Carnevale, V. On the Role of Water Density Fluctuations in the Inhibition of a Proton Channel. *Proc. Natl. Acad. Sci. U. S. A.* 2016, 113, E8359—E8368.
- (25) Geragotelis, A. D.; Wood, M. L.; Göddeke, H.; Hong, L.; Webster, P. D.; Wong, E. K.; Freites, J. A.; Tombola, F.; Tobias, D. J. Voltage-Dependent Structural Models of the Human Hv1 Proton Channel from Long-Timescale Molecular Dynamics Simulations. *Proc. Natl. Acad. Sci. U. S. A.* 2020, 117, 13490—13498.
- (26) Lee, M.; Bai, C.; Feliks, M.; Alhadeff, R.; Warshel, A. On the Control of the Proton Current in the Voltagegated Proton Channel Hv1. *Proc. Natl. Acad. Sci. U. S. A.* 2018, *115*, 10321–10326.
- (27) Van Keulen, S. C.; Gianti, E.; Carnevale, V.; Klein, M. L.; Rothlisberger, U.; Delemotte, L. Does Proton Conduction in the Voltage-Gated H+Channel HHv1 Involve Grotthuss-Like Hopping via Acidic Residues? *J. Phys. Chem. B* 2017, 121, 3340–3351.
- (28) Dudev, T.; Musset, B.; Morgan, D.; Cherny, V. V.; Smith, S. M. E.; Mazmanian, K.; Decoursey, T. E.; Lim, C. Selectivity Mechanism of the Voltage-Gated Proton Channel, Hv1. Sci. Rep. 2015, 5, 1–11.
- (29) Jardin, C.; Ohlwein, N.; Franzen, A.; Chaves, G.; Musset, B. The PH-Dependent Gating of the Human Voltage-Gated Proton Channel from Computational Simulations. *Phys. Chem. Chem. Phys.* **2022**, 24, 9964–9977.
- (30) Huang, Y.; Cai, Z.; Liu, T.; Shen, J. Mechanism of pH Sensing in the Human Voltage-Gated Proton Channel hHv1. *Bioarxiv* 2022, DOI: 10.1101/2022.12.07.519452 (accessed 8/14/2023), submitted 12/8/2022.
- (31) Berger, T. K.; Isacoff, E. Y. The Pore of the Voltage-Gated Proton Channel. *Neuron* 2011, 72, 991–1000.
- (32) Randolph, A. L.; Mokrab, Y.; Bennett, A. L.; Sansom, M. S. P.; Ramsey, I. S. Proton Currents Constrain Structural Models of Voltage Sensor Activation. *Elife* 2016, *5*, 1–29.
- (33) Sakata, S.; Kurokawa, T.; Nørholm, M. H. H.; Takagi, M.; Okochi, Y.; Von Heijne, G.; Okamura, Y. Functionality of the Voltage-Gated Proton Channel Truncated in S4. *Proc. Natl. Acad. Sci. U. S. A.* 2010, 107, 2313–2318.
- (34) Lazaridis, T.; Hummer, G. Classical Molecular Dynamics with Mobile Protons. J. Chem. Inf. Model. 2017, 57, 2833–2845.
- (35) Banh, R.; Cherny, V. V.; Morgan, D.; Musset, B.; Thomas, S.; Kulleperuma, K.; Smith, S. M. E.; Pomès, R.; DeCoursey, T. E. Hydrophobic Gasket Mutation Produces Gating Pore Currents in Closed Human Voltage-Gated Proton Channels. *Proc. Natl. Acad. Sci. U. S. A.* 2019, 116, 18951–18961.
- (36) Li, Q.; Wanderling, S.; Paduch, M.; Medovoy, D.; Singharoy, A.; Mcgreevy, R.; Villalba-Galea, C. A.; Hulse, R. E.; Roux, B.; Schulten, K.;

- et al. Structural Mechanism of Voltage-Dependent Gating in an Isolated Voltage-Sensing Domain. *Nat. Struct. Mol. Biol.* **2014**, *21*, 244–252.
- (37) Long, S. B.; Tao, X.; Campbell, E. B.; MacKinnon, R. Atomic Structure of a Voltage-Dependent K+ Channel in a Lipid Membrane-like Environment. *Nature* **2007**, *450*, 376—U3.
- (38) Webb, B.; Sali, A. Comparative Protein Structure Modeling Using MODELLER. Curr. Protoc. Bioinforma. 2016, 54, na.
- (39) Ismer, J.; Rose, A. S.; Tiemann, J. K. S.; Goede, A.; Preissner, R.; Hildebrand, P. W. SL2: An Interactive Webtool for Modeling of Missing Segments in Proteins. *Nucleic Acids Res.* **2016**, *44*, W390—W394.
- (40) Starace, D. M.; Stefani, E.; Bezanilla, F. Voltage-Dependent Proton Transport by the Voltage Sensor of the Shaker K+ Channel. *Neuron* 1997, 19, 1319–1327.
- (41) Tombola, F.; Pathak, M. M.; Isacoff, E. Y. Voltage-Sensing Arginines in a Potassium Channel Permeate and Occlude Cation-Selective Pores. *Neuron* **2005**, *45*, 379–388.
- (42) Wu, E. L.; Cheng, X.; Jo, S.; Rui, H.; Song, K. C.; Dávila-Contreras, E. M.; Qi, Y.; Lee, J.; Monje-Galvan, V.; Venable, R. M.; et al. CHARMM-GUI Membrane Builder toward Realistic Biological Membrane Simulations. *J. Comput. Chem.* 2014, 35, 1997–2004.
- (43) Lazaridis, T. Molecular Origins of Asymmetric Proton Conduction in the Influenza M2 Channel. *Biophys. J.* 2023, 122, 90–98.
- (44) Best, R. B.; Zhu, X.; Shim, J.; Lopes, P. E. M.; Mittal, J.; Feig, M.; MacKerell, A. D. Optimization of the Additive CHARMM All-Atom Protein Force Field Targeting Improved Sampling of the Backbone φ, ψ and Side-Chain X1 and X2 Dihedral Angles. J. Chem. Theory Comput. 2012, 8, 3257–3273.
- (45) Klauda, J. B.; Venable, R. M.; Freites, J. A.; O'Connor, J. W.; Tobias, D. J.; Mondragon-Ramirez, C.; Vorobyov, I.; MacKerell, A. D., Jr.; Pastor, R. W. Update of the CHARMM All-Atom Additive Force Field for Lipids: Validation on Six Lipid Types. *J. Phys. Chem. B* **2010**, 114, 7830—7843.
- (46) Essmann, U.; Perera, L.; Berkowitz, M. L.; Darden, T.; Lee, H.; Pedersen, L. G. A Smooth Particle Mesh Ewald Method. *J. Chem. Phys.* 1995, 103, 8577–8593.
- (47) Sagnella, D. E.; Voth, G. A. Structure and Dynamics of Hydronium in the Ion Channel Gramicidin A. *Biophys. J.* **1996**, 70, 2043–2051.
- (48) Brooks, B. R.; Brooks, C. L., 3rd; Mackerell, A. D., Jr.; Nilsson, L.; Petrella, R. J.; Roux, B.; Won, Y.; Archontis, G.; Bartels, C.; Boresch, S.; et al. CHARMM: The Biomolecular Simulation Program. *J. Comput. Chem.* 2009, 30, 1545–1614.
- (49) Mottamal, M.; Lazaridis, T. Voltage-Dependent Energetics of Alamethicin Monomers in the Membrane. *Biophys. Chem.* **2006**, 122, 50–57.
- (50) Decoursey, T. E. The Voltage-Gated Proton Channel: A Riddle, Wrapped in a Mystery, inside an Enigma. *Biochemistry* **2015**, *54*, 3250–3268.
- (51) Siemers, M.; Bondar, A. N. Interactive Interface for Graph-Based Analyses of Dynamic H-Bond Networks: Application to Spike Protein S. J. Chem. Inf. Model. 2021, 61, 2998—3014.
- (52) Lazaridis, T.; Sepehri, A. Amino Acid Deprotonation Rates from Classical Force Fields. *J. Chem. Phys.* **2022**, *157*, No. 085101.
- (53) Boytsov, D.; Brescia, S.; Chaves, G.; Koefler, S.; Hannesschlaeger, C.; Siligan, C.; Goessweiner-Mohr, N.; Musset, B.; Pohl, P. Trapped Pore Waters in the Open Proton Channel HV1. *Small* 2023, 19, e2205968.
- (54) Decoursey, T. E. Voltage-Gated Proton Channels: What's Next? J. Physiol. 2008, 586, 5305—5324.
- (55) Robinson, A. C.; Castañeda, C. A.; Schlessman, J. L.; García-Moreno, E. B. Structural and Thermodynamic Consequences of Burial of an Artificial Ion Pair in the Hydrophobic Interior of a Protein. *Proc. Natl. Acad. Sci. U. S. A.* 2014, 111, 11685–11690.
- (56) Starace, D. M.; Bezanilla, F. A Proton Pore in a Potassium Channel Voltage Sensor Reveals a Focused Electric Field. *Nature* **2004**, 427, 548–553.

## Recommended by ACS

#### Proton Release Reactions in the Inward H+ Pump NsXeR

Luiz Schubert, Joachim Heberle, et al.

SEPTEMBER 20, 2023

THE JOURNAL OF PHYSICAL CHEMISTRY B

READ [2]

# Arginine Residues Modulate the Membrane Interactions of pHLIP Peptides

Tomás F. D. Silva, Miguel Machuqueiro, et al.

JULY 03, 2023

JOURNAL OF CHEMICAL INFORMATION AND MODELING

READ 🗹

### Selective Unidirectional Transport of Protons in Sub-Nanoporous Membranes Inspired by the Influenza A M2 Channel for Nanofluidic Ionic Diodes

Haonan Qu, Haibing Li, et al.

OCTOBER 05, 2022

ACS APPLIED NANO MATERIALS

READ 🗗

## Aqueous Proton Transportation in Graphene-Based Nanochannels

Humin Duan, Le Shi, et al.

DECEMBER 02, 2022

LANGMUIR

READ C

Get More Suggestions >